Lipid Membranes Carrying Lipophilic Cholesterol-Based Oligonucleotides—Characterization and Application on Layer-by-Layer Coated Particles

Andreas Bunge,[†] Martin Loew,[‡] Paula Pescador,[†,§] Anna Arbuzova,[‡] Nicolai Brodersen,[||] Jing Kang,[⊥] Lars Dähne,[⊥] Jürgen Liebscher,[||] Andreas Herrmann,[‡] Gudrun Stengel,[#] and Daniel Huster*[,†]

Institute of Medical Physics and Biophysics, University of Leipzig, Härtelstr. 16-18, D-04107 Leipzig, Germany, Institute of Biology, Humboldt University Berlin, Invalidenstr. 42, D-10115 Berlin, Germany, Biosurfaces Unit, CIC biomaGUNE, Paseo Miramón 182, 20009 San Sebastián, Spain, Institute of Chemistry, Humboldt University Berlin, Brook-Taylor-Str. 2, D-12489 Berlin, Germany, Surflay Nanotec GmbH, Schwarzschildstr. 8, D-2489 Berlin, Germany, and Department of Chemistry and Biochemistry, University of Colorado, Boulder, Colorado 80309-0215

Received: July 17, 2009; Revised Manuscript Received: November 12, 2009

Cholesterol-based lipophilic oligonucleotides incorporated into lipid membranes were studied using solid-state NMR, differential scanning calorimetry, and fluorescence methods. Lipophilic oligonucleotides can be used to build nanotechnological structures on membrane surfaces, taking advantage of the specific Watson−Crick base pairing. We used a cholesteryl-TEG anchor first described by Pfeiffer and Höök (*J. Am. Chem. Soc.* **2004**, *126*, 10224−10225). The cholesterol-based anchor molecules were found to incorporate well into lipid membranes without disturbing the bilayer structure and dynamics. In contrast to cholesterol, which is known to induce significant condensation of the membrane lipids, the cholesteryl-TEG anchor does not display this property. When the cholesteryl-TEG moiety was covalently bound to an oligonucleotide, the resulting lipophilic DNA molecules inserted spontaneously into lipid membranes without altering their structure. The duplex formed by two complementary cholesteryl-TEG oligonucleotides had increased thermodynamic stability compared to the same oligonucleotides without the anchor, both in solution and incorporated into lipid membranes. Since the cholesteryl-TEG anchor lacks the characteristic properties of cholesterol, oligonucleotides modified with this anchor are equally distributed between liquid-disordered and liquid-ordered domains in "raft" forming membranes. As an example of an application of these lipophilic oligonucleotides, cholesteryl-TEG-DNA was incorporated into supported lipid bilayers formed on polyelectrolyte-coated silica microparticles. The modified oligonucleotides were stably inserted into the lipid membrane and retained their recognition properties, therefore enabling further functionalization of the particles.

Introduction

DNA oligonucleotides have recently achieved popularity as "intelligent glue" for various nanobiotechnological, pharmaceutical, and medical applications.[1−3] Due to their self-assembly and molecular recognition properties, oligonucleotides can serve as controllable and programmable building blocks for the precise spatial arrangement of biomolecules (such as proteins, ligands, or DNA), nanoparticles, cells, and other targets on artificial surfaces.[4] However, such systems often require harsh and not generally applicable surface chemistry procedures to effectively couple oligonucleotides to the solid support.

Alternatively, for the functionalization of biocompatible fluid surfaces such as lipid membranes, the covalent attachment of lipophilic modifications to oligonucleotides provides sufficient hydrophobic character for their spontaneous insertion into the bilayer, resulting in stable binding to the surface. In analogy to numerous cellular proteins and other biomolecules with covalently attached lipophilic modifications,[5−9] oligonucleotides have been coupled to cholesterol,[10−13] phospholipids,[14,15] α-tocopherol,[16,17] and alkyl chains.[18,19] Several studies have demonstrated the potential applications of these lipophilic oligonucleotides. Oligonucleotides with hydrophobic modifications have been used for tethering lipid vesicles to supported lipid bilayers,[20,21] for antisense strategy in gene therapy,[22] to mimic SNARE-mediated membrane fusion,[23] and to build supramolecular networks of soft colloids.[24] Controlled arrangement of multiple layers of vesicles on a spherical support provided by layer-by-layer (LbL)-coated colloids for release of reactants on demand has also been reported.[25]

With practical applications in mind, LbL-coated particles are an attractive platform for the development of controlled supramolecular architectures. In particular, much attention has been given to the possibility of using LbL-functionalized colloids as transport containers for targeted and effective cellular uptake of drugs, and in this context, intelligent surface modification strategies are needed. Specific recognition of biofunctionalized (i.e., with antibodies or peptides) LbL-coated particles by their respective receptors, resulting in subsequent binding or even internalization into target cells and release of encapsulated drugs on demand, represents substantial progress in the field of modern drug delivery systems.[26] Recently, it has been shown that supported lipid bilayers can be formed on LbL polyelectrolyte-

* Corresponding author. Phone: 49 (0) 341 97 15701. Fax: 49 (0) 341 97 15709. E-mail: daniel.huster@medizin.uni-leipzig.de.
[†] University of Leipzig.
[‡] Institute of Biology, Humboldt University Berlin.
[§] CIC biomaGUNE.
[||] Institute of Chemistry, Humboldt University Berlin.
[⊥] Surflay Nanotec GmbH.
[#] University of Colorado.

10.1021/jp9067747
Published on Web 12/03/2009

coated particles,[27] resulting in bilayer dynamic and structural properties that are comparable to those of free-standing membranes.[28,29] So far, binding of antibodies to the lipid membrane surface of LbL-coated particles has been realized via nonspecific electrostatic interactions.[27] The specific molecular recognition properties of complementary oligonucleotide pairs, one molecule covalently functionalized and the other as lipophilic oligonucleotide incorporated into LbL supported lipid bilayers, may provide a versatile alternative for the functionalization of lipid-coated particles with specific ligands or biomarkers. For this purpose, lipophilic oligonucleotides have to be inserted stably into lipid membranes by means of their hydrophobic modifications, but without significantly altering the bilayer structure or inducing formation of nonlamellar phases.

It may further be useful to obtain a lateral segregation of oligonucleotides in the membrane, for example, in lipid domains, which can be accomplished by using ternary ("raft-like") lipid mixtures. Depending on their lipophilic modification, oligonucleotides could incorporate with preference either into liquid-ordered (l_o) or into liquid-disordered (l_d) domains, as shown for lipidated peptides and proteins.[30−32] The l_o domains are rich in lipids with saturated chains, sphingolipids, and cholesterol, and show high acyl chain order. In l_d domains, the lipids are loosely packed, depleted of cholesterol, and enriched with phospholipids carrying unsaturated hydrocarbon chains. Detailed characterization of such ternary lipid mixtures has been reported elsewhere.[33−36] We have recently shown that oligonucleotides with α-tocopherol as lipophilic modification spontaneously incorporate into l_d domains.[16,17]

In this study, we have used oligonucleotides that are modified by covalent attachment of the cholesterol analogue cholesteryl-tri(ethylene glycol) (cholesteryl-TEG) and spontaneously incorporate into lipid membranes.[10,12] Cholesteryl-TEG-DNA is commercially available and was recently used by several groups to study hybridization-induced vesicle aggregation[11,37] and fusion,[23,38] as well as lateral diffusion of vesicles tethered to supported bilayers.[21] The lateral distribution of cholesteryl-TEG oligonucleotides was recently studied using giant unilamellar vesicles GUVs made of phosphatidylcholines with different acyl chain composition and cholesterol.[39] In solid−liquid phase-separated vesicles, all cholesteryl-TEG oligonucleotides were excluded from the solid phase.[39] In vesicles with liquid−liquid coexisting phases, a slightly higher partitioning into the liquid-ordered phase was observed for oligonucleotides with a single cholesteryl-TEG anchor. For a hybrid of two cholesteryl-TEG oligonucleotides or for oligonucleotides with two cholesterol anchors, this effect was even more pronounced.

It has been shown previously that single cholesterol motifs covalently attached to peptides provide adequate membrane anchorage, comparable to that of doubly palmitoylated molecules.[40] Using quarz crystal microbalance with dissipation (QCM-D) and supported bilayers, Pfeiffer and Höök found that the incorporation of oligonucleotides with a single cholesteryl-TEG anchor was reversible, whereas the incorporation of a hybrid with two cholesteryl-TEG anchors was almost irreversible.[10] In the present work, we also employed such a hybrid of two complementary oligonucleotides (27mer and 12mer) with cholesteryl-TEG at the 5′- or 3′-end of the strands and with the 3′-end of the 27mer available for hybridization with a labeled reporter oligonucleotide.

First, we studied membrane-associated cholesteryl-TEG using solid-state NMR and compared its properties with those of natural cholesterol, in terms of the effect on the lateral organization of lipid membranes, lipid packing density, and chain length.[41−43] We next characterized the behavior of membrane-associated cholesteryl-TEG-DNA by analyzing the duplex thermal stability and the influence on membrane morphology of lipophilic oligonucleotides, as well as their lateral distribution in ternary lipid mixtures. Finally, the successful functionalization of supported lipid membranes formed on LbL-coated particles with lipophilic oligonucleotides was demonstrated.

TABLE 1: Sequences of the Oligonucleotides Used[a]

oligo	sequence
O1	**cholesteryl-TEG**−5′-TCC-GTC-GTG-CCT-TAT-TTC-TGA-TGT-CCA-3′
O1*[b]	**cholesteryl-TEG**−5′-TCC-GTC-GTG-CCT-TAT-TTC-TTC-(FAM)GA-TGT-CCA-3′
O2	5′- AGG-CAC-GAC-GGA-3′−**TEG-cholesteryl**
O3	5′- TGG-ACA-TCA-GAA-ATA-3′
O3*[c]	(FAM)- 5′- TGG-ACA-TCA-GAA-ATA-3′
O4	5′-TCC-GTC-GTG-CCT-TAT-TTC-TGA-TGT-CCA-3′
O5	5′- AGG-CAC-GAC-GGA-3′

[a] O2 and O3 are complementary to O1; O4 and O5 have the same sequence as O1 and O2, respectively, but lack the cholesteryl-TEG modification. [b] Fluorescently labeled version of O1. [c] Fluorescently labeled version of O3.

Experimental Procedures

Materials. POPC (1-palmitoyl-2-oleoyl-*sn*-glycero-3-phosphocholine), POPC-d_{31} (1-palmitoyl-d_{31}-2-oleoyl-*sn*-glycero-3-phosphocholine), DOPC (1,2-dioleoyl-*sn*-glycero-3-phosphocholine), SSM (*N*-stearoyl-D-*erythro*-sphingosylphosphorylcholine), POPS (1-palmitoyl-2-oleoyl-*sn*-glycero-3-phospho-L-serine), Rh-DPPE (1,2-dipalmitoyl-*sn*-glycero-3-phosphoethanolamine-*N*-(lissamine rhodamine B sulfonyl, ammonium salt), and cholesterol (Chol) were purchased from Avanti Polar Lipids (Alabaster, AL). Lipids were used without further purification. Oligonucleotides with a covalently attached fluorophore (carboxyfluorescein, FAM) and cholesteryl-TEG-DNA were purchased from Eurogentec S.A. (Belgium). DNA oligonucleotides without fluorescent or lipophilic modifications were synthesized by BioTeZ (Berlin, Germany). Oligonucleotide sequences are given in Table 1. The monomer cholesteryl-TEG was obtained from MedProbe (Lund, Sweden) as a phosphoramidite; the compound was oxidized in 26% hydrogen peroxide, and the cyanoethyl group was cleaved off in a saturated ammonium hydroxide solution. Silica particles with a diameter of 3 μm were purchased from microparticles GmbH (Berlin, Germany). Poly(allylamine hydrochloride) (PAH, 700 000 g/mol) and poly(styrenesulfonate) (PSS, 700 000 g/mol) were obtained from Sigma-Aldrich.

Preparation of Lipid Membranes. For ^{2}H and ^{31}P NMR measurements of cholesteryl-TEG and cholesterol, 4/1 mol/mol mixtures of phospholipids and sterols were prepared in a chloroform/methanol mixture (1/1 v/v). The solvent was removed by rotary evaporation, and the resulting lipid film was redissolved in cyclohexane and lyophilized overnight to obtain a fluffy powder. Samples were hydrated with 40 wt % water and equilibrated by 10 freeze−thaw cycles and gentle centrifugation to obtain multilamellar vesicles (MLVs). The lipid/water dispersions were transferred into 4 mm high resolution MAS rotors fitted with spherical Kel-F inserts for liquid samples for static ^{31}P and ^{2}H NMR experiments.

For ^{2}H and ^{31}P NMR measurements of membrane-associated cholesteryl-TEG-DNA, phospholipids were dissolved in a chloroform/methanol mixture (1/1 v/v) followed by rotary evaporation. The resulting homogeneous lipid film was hydrated to 20 mM with water and equilibrated by 10 freeze−thaw cycles

and gentle centrifugation. Subsequently, large unilamellar vesicles (LUVs) were formed by subjecting this suspension to 10 freeze−thaw cycles and extrusion[44] 10 times through two stacked polycarbonate filters (Nucleopore GmbH, Tübingen, Germany) of 100 nm pore diameter using an extruder (Lipex Biomembranes Inc., Vancouver, Canada). Aliquots of cholesteryl-TEG-DNA O1 and O2 were added to POPC LUVs at an O1 to lipid molar ratio of 1:130, and after an incubation time of 30 min, the complementary O3 strand was also added to the solution. The molar O1:O2:O3 ratio was 1:1:1. The solvent was removed by lyophilization for 24 h to obtain a powder with a homogeneous distribution of lipids and oligonucleotides. Samples were hydrated with 80 wt % buffer (100 mM NaCl, 10 mM Tris, pH 7.4) and equilibrated by 10 freeze−thaw cycles and gentle centrifugation.

For DSC measurements, LUVs were prepared in 100 mM NaCl, 10 mM Tris, pH 7.4, at a lipid concentration of 1 mg/mL, followed by the sequential incorporation of O1, O2, and O3.

For preparation of lipid membranes supported on LbL-coated particles, a POPS/POPC (1/1 mol/mol) lipid film was obtained by rotary evaporation of the phospholipid mixture in chloroform. The lipid film was hydrated to 6.5 mM in phosphate buffer (1 mM Na_2HPO_4, 100 mM NaCl, 0.27 mM KCl, pH 7.4). Small unilamellar vesicles (SUVs) were obtained by extrusion through polycarbonate membrane filters with a pore diameter of 50 nm (Avestin Inc., Canada).

Giant unilamellar vesicles (GUVs) were prepared by the electroformation method[45] in a titanium chamber. A 100 nmol aliquot of a lipid mixture in chloroform was spotted onto a titanium plate and heated to 50 °C to remove the solvent. Traces of chloroform were removed under vacuum for at least 1 h. After sealing, the titanium chamber was filled with 1 mL of sucrose buffer (250 mM sucrose, 10 mM HEPES, pH 7.4). An alternating electrical field of 10 Hz, rising from 0.02 to 1.1 V in the first 30 min, was applied for 150 min, followed by 30 min of 4 Hz and 1.3 V to detach the formed liposomes. The process was carried out at 50−60 °C. Two lipid mixtures were used: (1) DOPC/SSM/Chol (1/1/1 molar ratios); (2) DOPC/SSM/Chol/POPS (1/1/1/1 molar ratios). In mixtures, 0.1 mol % Rh-DPPE was used as a marker for liquid-disordered domains.[46]

A 20 μL portion of GUV solution was mixed with 80 μL of a microscopy buffer (see below) and 0.13 μL of 10 μM lipophilic oligonucleotides (lipophilic oligonucleotide to lipid molar ratio of 1:3000) and incubated for 15 min at room temperature. As a microscopy buffer, glucose buffer (280 mM glucose, 10 mM HEPES, pH 7.4), PBS buffer (10.1 mM Na_2HPO_4, 1.8 mM NaH_2PO_4, 137 mM NaCl, 2.7 mM KCl, pH 7.4), or mixtures of both with different ionic strengths were used.

Polyelectrolyte Multilayer Coating. Silica particles were coated with seven polyelectrolyte layers, alternating between positively charged PAH and negatively charged PSS. 1 mg/mL solutions of PAH or PSS in 500 mM NaCl were used for coating. Starting with PAH, each layer was allowed to adsorb for 10 min at room temperature under constant shaking, followed by three centrifugation/redispersion cycles in 100 mM NaCl to remove excess polyelectrolyte.

Preparation of Supported Membranes. Supported lipid bilayers were formed by incubation of lipid SUVs with the LbL polyelectrolyte-coated particles for 120 min in phosphate buffer (1 mM Na_2HPO_4, 100 mM NaCl, 0.27 mM KCl, pH 7.4) at 37 °C with constant stirring. The lipid concentration in the SUV coating solution was 0.65 mM, with a vesicle/particle ratio (the ratio between the surface areas of vesicles and particles, as defined by Carmona-Ribeiro et al.[47]) of $A_V/A_P = 500$, assuming 0.66 nm^2 per lipid monomer. After coating, five washing steps were performed in phosphate buffer to remove excess lipid. The particles were then washed two times in 100 mM NaCl and finally resuspended in HEPES buffer (10 mM HEPES, 100 mM NaCl, pH 7.2).

The lipid-coated colloids were next successively incubated with the lipophilic oligonucleotides O1 and O2 and the fluorescence-labeled oligonucleotide O3*, complementary to the 3′-end, with five intermediate washing steps in HEPES buffer between incubations. Aliquots of the oligonucleotides were diluted in HEPES buffer before adding the particles, giving the final molar ratio of oligonucleotide to lipid of 1:130. Incubation steps were performed for 30 min at 37 °C under constant stirring. After the final incubation with O3*, the particles were washed five times and resuspended in HEPES buffer.

NMR Measurements. Static ^{31}P NMR spectra of the MLVs were acquired on a Bruker DRX600 NMR spectrometer (Bruker BioSpin, Rheinstetten, Germany) at a resonance frequency of 242.9 MHz using a Hahn-echo pulse sequence. A ^{31}P 90° pulse length of 7 μs, a Hahn-echo delay of 50 μs, a spectral width of 100 kHz, and a recycle delay of 3 s were used. Continuous-wave proton decoupling was applied during signal acquisition. Phosphoric acid was used as an external reference for the ^{31}P NMR chemical shift. Spectra were simulated using a program written in MathCad 2001 (MathSoft, Cambridge, USA), considering an elliptical distribution of phospholipids due to macroscopic alignment of the vesicles in the external magnetic field.

^{2}H NMR spectra were recorded on a Bruker Avance 750 NMR spectrometer (Bruker BioSpin, Rheinstetten, Germany) at a resonance frequency of 115.1 MHz for ^{2}H, using a single channel solids probe with a 5 mm solenoid coil. The ^{2}H NMR spectra were accumulated using the quadrupolar echo sequence[48] and a relaxation delay of 1 s. The two 4 μs $\pi/2$ pulses were separated by a 60 μs delay. Typically, 16 k scans with a spectral width of 500 kHz were acquired. For all experiments, the carrier frequency of the spectrometer was placed in the center of the spectrum. The free induction decays were left-shifted after acquisition to initiate Fourier transformation on top of the quadrupolar echo.

^{2}H NMR spectra were dePaked,[49] and smoothed order parameters[50] for each methylene group in the chain were determined from the observed quadrupolar splittings $\Delta\nu_Q^{(i)}$ for the ith chain segment according to

$$|\Delta\nu_Q^{(i)}| = \frac{3}{4}\chi_Q|S_{CD}^{(i)}| \quad (1)$$

where $\chi_Q = e^2qQ/h$ represents the quadrupolar coupling constant (167 kHz for the C−^{2}H bond), $S_{CD}^i = {}^1/_2\langle 3\cos^2\theta_i - 1\rangle$ is the segmental order parameter, and θ is the angle between the bilayer director and the external magnetic field B_0.

The Pake doublets were assigned starting from the terminal methyl group exhibiting the smallest quadrupolar splitting. The methylene groups were assigned successively according to their increasing quadrupolar splittings. The smoothed order parameter profiles were determined from the observed quadrupolar splittings, as described in detail in Huster et al.[51] Average order parameters were calculated by adding all chain order parameters and dividing them by the number of methylene and methyl groups in the chain. The chain extension L_C^* can be estimated by projection of the averaged length of the carbon segments on

the bilayer normal and summation over successional carbon segments.[52,53]

For the ^{2}H NMR relaxation studies, a phase-sensitive inversion recovery quadrupolar echo pulse sequence was used to obtain the spin−lattice relaxation time T_{1Z}. The ^{2}H NMR spectra were accumulated using a relaxation delay of 2 s. Spectral simulations of the ^{2}H NMR spectra were carried out to obtain the individual T_{1Z} by using a program written in MathCad 2001 (MathSoft, Cambridge, USA).

Differential Scanning Calorimetry (DSC). DSC measurements were carried out on a MicroCal VP-DSC calorimeter (MicroCal, Inc., Northampton, MA) using a scan rate of 60 K/h. Heating scans from 5 to 110 °C were performed. For measurements of oligonucleotides in the presence of lipid vesicles, the reference cell was filled with liposomes using the same concentration of lipids as in the sample cell. The lipid concentration used for DSC measurements was 1 mg/mL.

Confocal Fluorescence Microscopy. All images were acquired with an inverted IX81 fluorescence microscope equipped with a FluoView 1000 scan head (Olympus, Tokyo, Japan) and a 60× (N.A. 1.35) oil-immersion objective at 25 °C. FAM was excited with the 488 nm laser line of an Ar-ion laser, and rhodamine was excited with a 559 nm laser diode. Images were obtained in sequential scanning mode to avoid spectral overlap. Emitted light was separated from excitation light with a dichroic mirror reflecting light with a wavelength of 405, 488, 559, and 635 nm (excitation dichroic mirror FV10-DMVBYR, Olympus). Fluorescence emission of FAM-labeled samples was recorded up to 547 nm. Scattering of the excitation light was negligible at the plane of study. For rhodamine-labeled samples, the emission was recorded between 580 and 680 nm. Rhodamine fluorescence was separated from FAM fluorescence using a dichroic mirror transmitting light above 560 nm. The distribution of oligonucleotides between the l_o and l_d domains was calculated from the FAM fluorescence intensities in the presence of lipid membranes. Liquid-disordered domains were identified by rhodamine fluorescence, since Rh-DPPE spontaneously incorporates into those domains.[46] Only GUVs showing a separation of l_o and l_d domains were analyzed. Fluorescence intensities were determined at two points of the membranes for both the l_o and l_d domains and were averaged separately. FAM intensities of oligonucleotides localized in the l_d phase (I_d) were corrected using eq 2:

$$I_{c/d} = I_d/(1 - ET) \quad (2)$$

where $I_{c/d}$ is the corrected intensity of FAM in the l_d phase and ET is the energy transfer efficiency calculated from FLIM data (see below). The fraction of lipophilic oligonucleotides in the l_o phase (f_o) was obtained using eq 3:

$$f_o = I_o/(I_o + I_{c/d}) \quad (3)$$

where I_o is the intensity of FAM in the l_o phase.

Fluorescence Lifetime Imaging Microscopy (FLIM). As the fluorescence emission spectrum of FAM overlaps with the absorption spectrum of rhodamine, FAM fluorescence might be reduced by Förster resonance energy transfer (FRET). To quantify FRET and correct the measured FAM intensities, FLIM was performed. Images were acquired using the time-resolved LSM Upgrade Kit from PicoQuant (Berlin, Germany) on the microscope. FAM was excited at 470 nm using a pulsed laser diode. The fluorescence was detected by a single photon avalanche photodiode with a 540 ± 20 nm filter. Data were analyzed using the SymPhoTime software (PicoQuant). FLIM pictures were accumulated for 60 s. The best two-exponential fit to the averaged fluorescence decay curve as judged by visual examination of the residuals was used. A so-called "tail-fit" was performed, meaning that only the part which was not affected by the instrument response function (IRF) was used for the fit. A typical FLIM image and a typical fluorescence decay curve including the best fit and the residuals are presented in the Supporting Information (Figures S1 and S2). For the calculation of energy transfer efficiency (ET), the amplitude weighted average lifetime $\langle\tau\rangle$ was used (eq 4):[54]

$$\langle\tau\rangle = \frac{\alpha_1\tau_1 + \alpha_2\tau_2}{\alpha_1 + \alpha_2} \quad (4)$$

where τ_1 and τ_2 are the first and second lifetime components and α_1 and α_2 are the corresponding amplitudes. ET was calculated using eq 5:[54]

$$ET = 1 - \langle\tau_{DA}\rangle/\langle\tau_D\rangle \quad (5)$$

where $\langle\tau_D\rangle$ is the amplitude weighted average fluorescence lifetime of the donor in the absence of an acceptor (lifetime of FAM in the membranes without Rh-DPPE) and $\langle\tau_{DA}\rangle$ is the amplitude weighted fluorescence lifetime of the donor in the presence of the acceptor, Rh-DPPE, which is constrained to the l_d domain.

Flow Cytometry. Flow cytometry was performed on a Becton Dickinson FACScalibur flow cytometer using an excitation wavelength of 488 nm. For each sample, 10 000 single colloids were measured. The data were analyzed using the WinMDI v2.8 software.

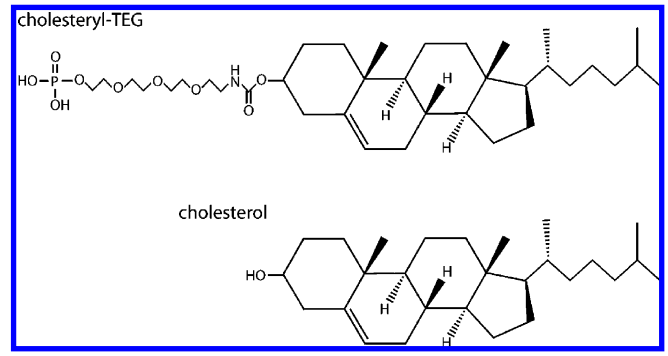

Figure 1. Chemical structures of cholesteryl-TEG and cholesterol.

Results

Characterization of Cholesteryl-TEG. First, cholesteryl-TEG, the membrane anchor moiety of the cholesteryl-TEG-DNA, was characterized using ^{31}P and ^{2}H solid-state NMR spectroscopy. ^{2}H and ^{31}P NMR are very sensitive tools to study the lateral organization, packing, and phase behavior of pure lipid bilayers,[55−60] as well as in the presence of lipophilic nucleosides and oligonucleotides.[16,61,62] The hydrophilic headgroup of cholesteryl-TEG is triethylene glycol with a covalently attached phosphate group. The membrane anchorage of the whole molecule was achieved through the cholesterol moiety (Figure 1). On the basis of the NMR measurements, the biophysical properties of cholesteryl-TEG were compared with those of natural cholesterol.

A ^{31}P NMR spectrum of POPC/cholesteryl-TEG (4/1, mol/mol) membranes is shown in Figure 2A. The general anisotropic ^{31}P line shape of phospholipids in a lamellar phase is characterized by a major peak in the high-field region and a low-field shoulder. The spectrum of the POPC/cholesteryl-TEG sample represents a superposition of two elements: first, an anisotropic

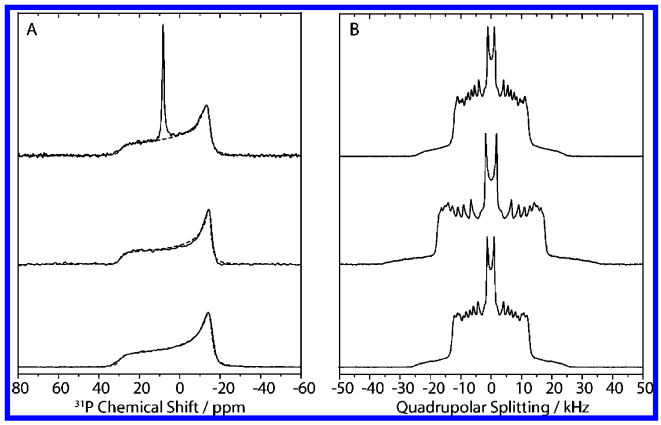

Figure 2. Proton-decoupled 242.9 MHz ^{31}P NMR spectra of POPC (A) and ^{2}H NMR (B) spectra of POPC-d_{31} bilayers in the absence and in the presence of cholesteryl-TEG or cholesterol, respectively. The spectra shown refer to 4/1 POPC/cholesteryl-TEG (top), 4/1 POPC/Chol (middle), and pure POPC membranes (bottom) recorded at 303 K, at a water content of 40 wt %. The dashed lines indicate the simulated ^{31}P NMR spectra of POPC used to fit the experimental line shape (parameters summarized in Table 2).

TABLE 2: Chemical Shift Anisotropies, $\Delta\sigma$; Average Order Parameters, S_{av}; and Average Chain Lengths of POPC, $\langle L_C^* \rangle$, in the Presence of Cholesteryl-TEG and Cholesterol, Determined from ^{31}P and ^{2}H NMR Spectra

sample	$\Delta\sigma$/ppm	S_{av}	$\langle L_C^* \rangle$/Å
POPC/cholesteryl-TEG	43.7	0.146	11.2
POPC/Chol	44.5	0.223	13.3
POPC	45.2	0.153	11.5

line shape indicative of an axially symmetric chemical shift tensor, characteristic of the liquid-crystalline lamellar phase state of the membrane, and second, an additional isotropic line at 7.87 ppm of 1.0 ppm width.

The chemical shift difference between the low- and high-field edges of the anisotropic ^{31}P NMR spectra is termed chemical shift anisotropy, $\Delta\sigma$, and is related to the orientation and dynamics of the phosphate group of the phospholipids. Compared to the value obtained for POPC membranes, a small decrease in $\Delta\sigma$ was observed in the presence of cholesteryl-TEG. ^{31}P chemical shift anisotropy values of POPC were obtained by using best-fit simulations of the spectrum (as shown in Figure 2 and summarized in Table 2).

The isotropic line in the ^{31}P NMR spectrum could be attributed to the cholesteryl-TEG phosphates, indicating a very mobile polar part of the sterol analogue. The ratio between the integrals of the anisotropic and isotropic lines roughly corresponds to the correct mixing ratio of phospholipid to cholesteryl-TEG. In the presence of cholesterol, ^{31}P NMR spectra are very similar to those of pure POPC membranes, with a slight reduction of the chemical shift anisotropy. This agrees with previous findings that cholesterol only marginally alters the orientation and mobility of the phospholipid headgroups.[63]

To compare the influence of cholesteryl-TEG with that of cholesterol on the lipid chain packing properties of the membranes, ^{2}H NMR experiments were conducted. The ^{2}H NMR powder spectra of POPC-d_{31} (deuterated palmitoyl chain) in the presence and absence of cholesteryl-TEG are quite similar and are characterized by the superposition of multiple Pake doublets (Figure 2B), showing the following elements: one intense doublet that can be assigned to the terminal methyl groups, exhibiting the smallest quadrupolar splitting; five well resolved doublets of methylene groups 15−11; and a plateau region arising from the carbons 2−10, which cannot be resolved. There is no indication of the formation of highly curved phospholipid structures induced by cholesteryl-TEG, since ^{2}H NMR spectra show no isotropic signal. Spectra of POPC-d_{31} in the presence of cholesterol feature larger quadrupolar splittings for all of the respective doublets. Smoothed order parameter profiles were extracted from ^{2}H NMR spectra (Figure 3). Cholesteryl-TEG slightly reduced the order parameters of lipid membranes compared to pure phospholipid bilayers, indicating that the molecules are well incorporated into the membrane without large alterations in the packing density of the phospholipids. In contrast, addition of cholesterol to POPC membranes strongly increased the order parameters by modulating the packing of the lipids and thus increasing the bilayer thickness, what is also known as the condensation effect.[64] Average order parameters and calculated chain extents[65] are given in Table 2.

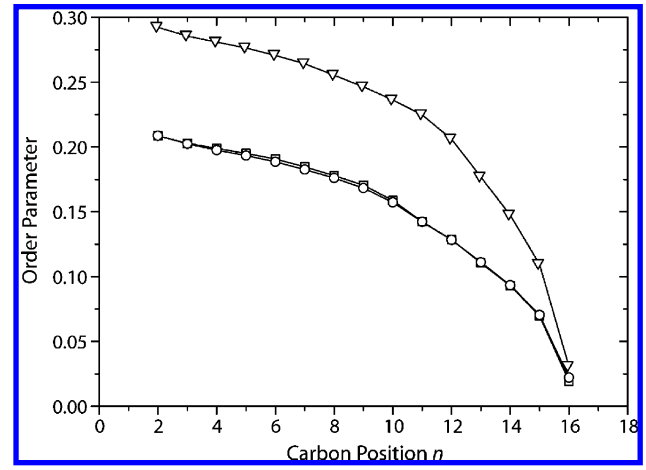

Figure 3. Smoothed chain order parameter profiles calculated from the ^{2}H NMR spectra of 4/1 POPC-d_{31}/cholesteryl-TEG (○), 4/1 POPC-d_{31}/Chol (▽), and pure POPC-d_{31} membranes (□). Lines are drawn to guide the eye.

To provide information about the lipid chain dynamics, ^{2}H NMR spin−lattice relaxation measurements were performed. For each peak doublet in the static ^{2}H NMR powder spectra, the Zeeman order longitudinal relaxation time (T_{1Z}) was determined in an inversion recovery experiment. The dependence of longitudinal relaxation rate, $R_{1Z} = 1/T_{1Z}$, with the squared order parameters for each individual methylene and methyl group of the saturated acyl chains in phospholipid membranes typically shows a linear dependence.[65,66] The slope of such a square-law plot is a measure for the elastic properties of the lipid membrane, and is inversely related to the softness of the membrane.[67] The square-law plot of POPC-d_{31} membranes shows a relatively linear dependence (Figure 4), in agreement with previously published data.[61] In the presence of cholesteryl-TEG, a slightly increased slope was observed, indicating softening of the lipid membrane. In contrast, addition of cholesterol to POPC-d_{31} membranes leads to a much shallower slope, reflecting a decrease in the elasticity of the lipid bilayer.

Characterization of Membrane Associated Cholesteryl-TEG-DNA. Second, membrane-associated cholesteryl-TEG-DNA oligonucleotides (Table 1) were characterized using ^{31}P and ^{2}H NMR spectroscopy and with differential scanning calorimetry (DSC). Cholesteryl-TEG-DNA spontaneously incorporates into lipid bilayers.[10] It has also been shown that lipophilic oligonucleotides can hybridize with cDNA strands, forming Watson−Crick base pairs.[16]

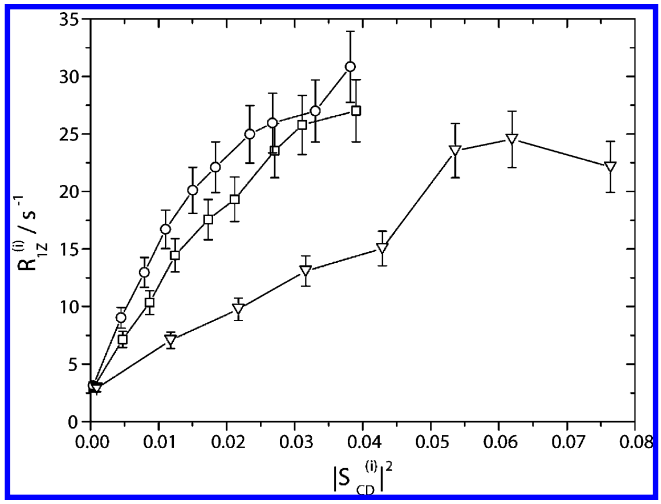

Figure 4. Square-law plots of 4/1 POPC-d_{31}/cholesteryl-TEG (○), 4/1 POPC-d_{31}/Chol (▽), and pure POPC-d_{31} membranes (□). Square law plots correlate the segmental spin−lattice relaxation rate with the corresponding segmental order parameter squared. Lines are drawn to guide the eye.

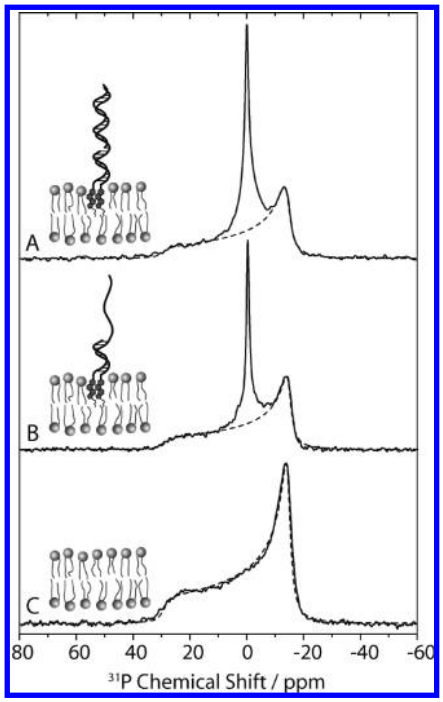

Figure 5. Proton-decoupled 242.9 MHz ^{31}P NMR spectra of POPC bilayers in the presence of O1/O2/O3 (A) and O1/O2 (B) and for pure POPC membranes (C) recorded at 303 K, at a molar ratio of oligonucleotides to phospholipids of 1/130 and 80 wt % buffer solution (100 mM NaCl, 10 mM Tris, pH 7.4). The dashed lines show the simulated ^{31}P NMR spectra of POPC used to fit the experimental line shape (see Table 3).

The ^{31}P NMR spectra of POPC membranes in the presence of double-stranded cholesteryl-TEG-DNA O1/O2/O3 or O1/O2 are shown in Figure 5A,B. The spectra show a superposition of an anisotropic line shape, indicative of the liquid-crystalline lamellar phase state of the membrane, and an isotropic line at −0.13 ppm of ∼1.3 ppm width related to the phosphate groups of the oligonucleotides. The corresponding chemical shift anisotropy values, $\Delta\sigma$, are listed in Table 3.

Looking only at the isotropic signal, the line shape of the spectrum for O1/O2 (Figure 5B) shows two superimposed components: a relatively broad element on the bottom, indicative of a more rigid part of the oligonucleotide (the helical double-stranded part of the duplex), and the narrow line corresponding to the free 3′-end of O1 (free 12mer), showing higher dynamics. Addition of an oligonucleotide complementary to the free 3′-end led to an increase in width of the isotropic peak at −0.28 to 2 ppm, indicating a higher rigidity of the DNA molecules due to the formation of a helix over the full length of O1 (Figure 5A). However, a quantification of these differences is not possible on the basis of the ^{31}P NMR spectra only, as the line broadening effects are due to both static and dynamic contributions. No alterations in the ^{31}P NMR chemical shift anisotropy of the lipid head groups were observed.

TABLE 3: Chemical Shift Anisotropies, $\Delta\sigma$; Width of Isotropic Peaks in ^{31}P NMR Spectra; Average Order Parameters, S_{av}; and Average Chain Lengths of POPC, $\langle L_C^* \rangle$, in the Presence of Cholesteryl-TEG-DNA, Determined from ^{31}P and ^{2}H NMR Spectra Measured at 303 K and 80 wt % Buffer Solution (100 mM NaCl, 10 mM Tris, pH 7.4)[a]

sample	$\Delta\sigma$/ppm	width of isotropic peak/ppm	S_{av}	$\langle L_C^* \rangle$/Å
POPC/O1/O2/O3	43.8	2.0	nt	nt
POPC/O1/O2	43.8	1.3	0.154	11.5
POPC	44.4		0.152	11.4

[a] nt = not tested.

However, the isotropic line could also be related to highly curved phospholipid structures induced by the incorporation of O1/O2. To rule this out, ^{2}H NMR spectra of POPC-d_{31} with and without addition of oligonucleotides were accumulated. In these measurements, where only lipids contributed to the ^{2}H NMR spectra, only a negligible isotropic signal was found at 0 kHz, proving that the insertion of nucleotides did not lead to formation of highly curved phospholipid structures (Figure 6).

In the presence of O1/O2, the order parameters for the palmitoyl chain of POPC calculated from the ^{2}H NMR spectra are very similar (Figure 6), indicating that essentially no membrane disturbance is imposed by the insertion of the cholesteryl-TEG-DNA.

The thermal stability of cholesterol-modified oligonucleotide duplexes was studied by DSC. This technique is an excellent tool to characterize thermally induced dissociation of oligonucleotide duplexes.[68,69] First, we measured the melting curves of nonmodified oligonucleotides O4 and O5, which are analogues of O1 and O2 but lacking the membrane anchor, in the presence and absence of an oligonucleotide complementary to the free 3′-end (O3) (Figure 7A). A melting curve with two peaks was observed for O4/O5/O3 double-stranded DNA (black). This can be explained by the separate melting of O4/O5 at 61.4 °C (red, measured) and of O3/O4 at 53.4 °C (green, subtracted). Melting of the shorter duplex O4/O5 occurred at a higher temperature compared to O3/O4 due to its higher GC content, whereas the latter showed larger cooperativity of the helix-to-coil transition, as revealed by the smaller width of the individual thermogram. The melting temperature of these DNA duplexes was the same in control measurements performed in the presence of POPC vesicles (data not shown).

Cholesterol-modified oligonucleotides showed a different melting behavior. In measurements with lipophilic oligonucleotides incorporated into POPC liposomes, the duplex formed by O1 and the oligonucleotide covering its 3′ free end (O3) still melts at 53.4 °C; i.e., the melting temperature of this duplex is not affected by the proximity of the lipid membrane. In contrast, the duplex O1/O2 shows an increased melting tem-

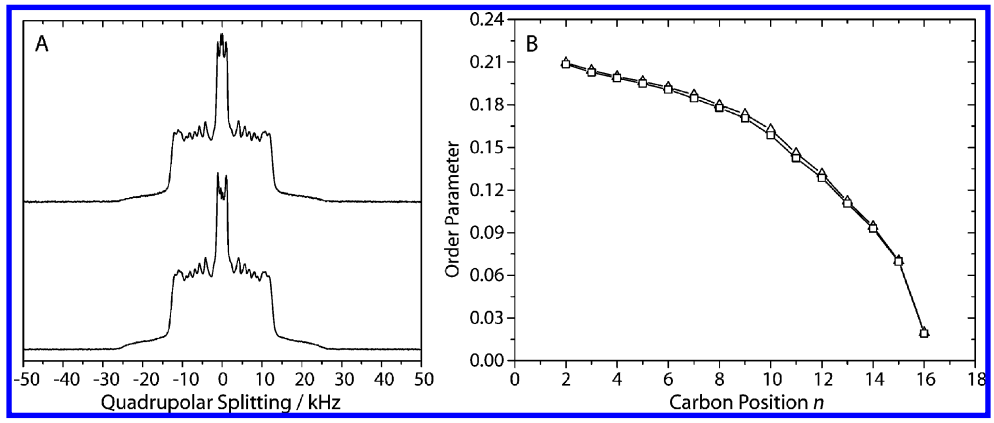

Figure 6. (A) ^{2}H NMR spectra of POPC-d_{31} lipid bilayers with (top) and without (bottom) O1/O2 (1/1 mol/mol) at a 1/130 O1/lipid molar ratio. (B) ^{2}H NMR order parameter profiles of POPC-d_{31} multilamellar vesicles in the presence (△) and absence (□) of O1/O2 (1/1 mol/mol). Measurements were conducted at 303 K with 80 wt % buffer (100 mM NaCl, 10 mM Tris, pH 7.4).

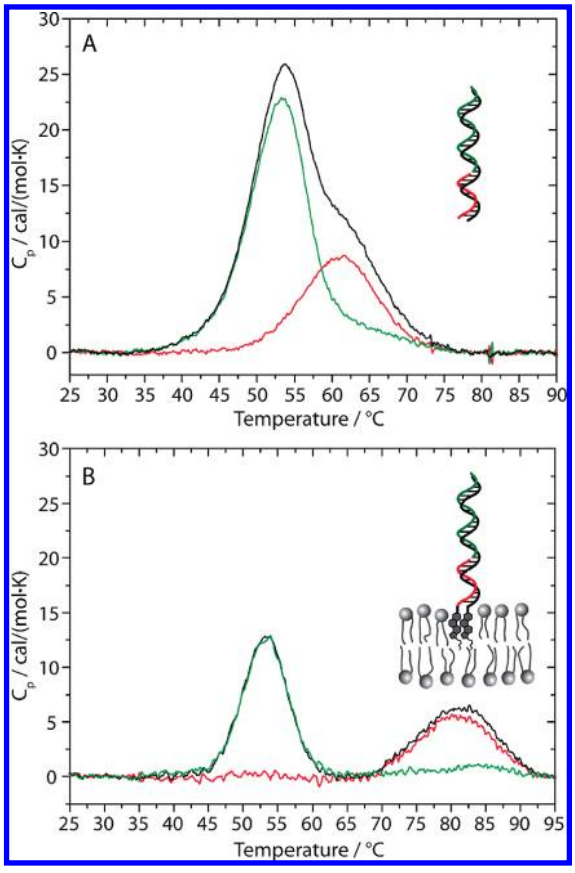

Figure 7. DSC thermograms. (A) O4/O5 (1/1 mol/mol) (red) and O4/O5/O3 (1/1/1 mol/mol/mol) (black) in buffer solution. (B) O1/O2 (1/1 mol/mol) (red) and O1/O2/O3 (1/1/1 mol/mol/mol) (black) attached to POPC vesicles, incorporated at a O1/POPC molar ratio of 1/300 and at the same oligonucleotide concentration used in part A. The green lines (difference) are obtained by subtracting the red curves from the black curves in each panel. The buffer solution was 100 mM NaCl, 10 mM Tris, pH 7.4.

perature of 81.2 °C (Figure 7B), in good agreement with Letsinger et al., who observed in dilute aqueous media "synergism for hydrophobic and basepairing/base-stacking interactions in stabilizing" of the duplex.[70] Cholesterol-modified oligonucleotides in buffer solution in the absence of lipid membranes also showed a higher melting temperature of 78.4 °C, with the duplex at the 3′ free end melting at 53.4 °C (data not shown). This can also be attributed to the hydrophobic attraction keeping the two cholesterols together and therefore stabilizing the duplex O1/O2.

Lateral Organization of Membrane-Associated Cholesteryl-TEG-DNA. Third, to study the lateral arrangement of cholesteryl-TEG-DNA in lipid membranes, different combinations of FAM-labeled and nonlabeled lipophilic oligonucleotides (O1*, O1*/O2, or O1/O2/O3*, added sequentially for duplex formation) were incorporated into GUVs made from a 1/1/1 DOPC/SSM/Chol lipid mixture. GUVs with this composition have been shown to form microscopically visible liquid-ordered and liquid-disordered domains.[71] To visualize domains, GUVs contained 0.1 mol % Rh-DPPE as a marker for liquid-disordered domains.[46] Significant amounts of either the single cholesteryl-TEG-DNA (O1*) or hybrids of two complementary cholesteryl-TEG-DNAs (O1*/O2 or O1/O2/O3*) were detected on GUVs membranes. On the basis of NMR and DCS results, we assume that O1 hybridized with O2 to form DNA duplexes. As seen in Figure 8 for the O1/O2/O3* complex, confocal microscopy images showed that the oligonucleotides were equally distributed in the liquid-ordered and liquid-disordered domains. FLIM measurements revealed differences between fluorescence lifetimes of FAM-labeled oligonucleotides in the liquid-ordered and liquid-disordered domains (Table 4). A slightly lower FAM fluorescence and a shorter fluorescence lifetime of FAM in the liquid-disordered domain is due to FRET between the FAM and rhodamine. After correction of the intensities, no significant difference between the lateral distribution of the single cholesteryl-TEG-DNA (O1*) and hybrids of two complementary cholesteryl-TEG-DNAs (O1*/O2 or O1/O2/O3*) was observed. The decreasing FRET efficiency in the order from O1* to O1*/O2 and to O1/O2/O3* (see Table 4) is consistent with the increasing distance between the FAM label on the oligonucleotides and the acceptor rhodamine in the membrane, due to the formation of a rigid DNA duplex. These data also support our assumption about the formation of O1*/O2 duplexes.

In PBS buffer (137 mM NaCl), the incorporation of POPS into the lipid mixture (1/1/1/1 DOPC/POPS/SSM/Chol) did not affect the lateral distribution of lipophilic oligonucleotides, either for O1* or for O1/O2/O3* (O1/O2 not tested). This is in spite of the fact that POPS, as a lipid with one unsaturated chain, is localized preferentially in l_d domains. The incorporation and lateral distribution of O1* in POPS-containing GUVs was also tested at lower ionic strengths. The length of the cholesteryl-TEG anchor is about 2−3 nm. As hydrophobic interactions are short-ranged, the anchor should come in close contact with the membrane in order to insert. In the experiments with lower ionic strength at an estimated Debye length between 5 and 10 nm, the long-range electrostatic repulsion between negatively charged

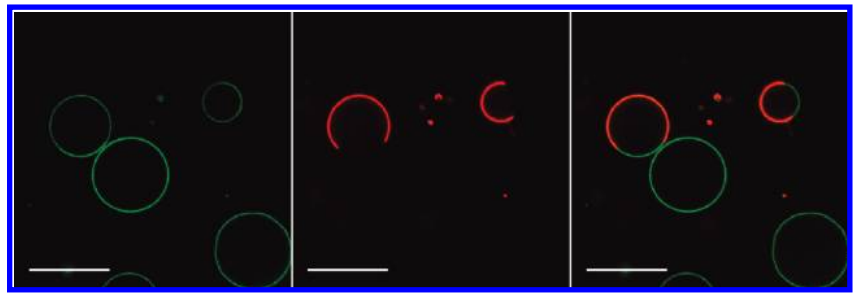

Figure 8. Confocal images of GUVs (1:1:1 DOPC/SSM/cholesterol, 0.1 mol % Rh-DPPE) with incorporated complex O1/O2/O3*, in PBS buffer. The FAM fluorescence (green) of O3* is equally distributed over the vesicle (left image), while the red fluorescence of Rh-DPPE is constrained to the l_d domains (middle image). The right images represent the overlay of both images. The bars correspond to 20 μm.

TABLE 4: Fraction of Oligonucleotides Partitioning into l_o Domains of DOPC/SSM/Chol GUVs, f_o[a]

oligonucleotides	f_o	$\langle\tau_{DA}\rangle$/ns	$\langle\tau_D\rangle$/ns	ET (FAM-Rh)
O1*	0.47 ± 0.03	3.39 ± 0.04	4.05 ± 0.03	0.16 ± 0.01
O1*/O2	0.50 ± 0.05	3.36 ± 0.11	3.83 ± 0.04	0.12 ± 0.03
O1/O2/O3*	0.48 ± 0.06	3.66 ± 0.03	3.96 ± 0.03	0.08 ± 0.02

[a] The data was obtained by analyzing 20−30 GUVs for each preparation. FRET efficiency values, ET, were calculated from amplitude weighted fluorescence lifetimes of FAM in l_d domains $\langle\tau_{DA}\rangle$ and in l_o domains $\langle\tau_D\rangle$ obtained by FLIM measurements. Data are presented with standard errors.

oligonucleotide and negatively charged lipid membrane prevented the hydrophobic anchor from coming close enough to integrate into the membrane: almost no incorporation of O1* was observed. In buffers with higher ionic strength (Debye length 1−2 nm), O1* incorporated into negatively charged GUVs and was equally distributed in both l_o and l_d phases, the same as in the zwitterionic membranes. This is a relevant finding for the subsequent functionalization of supported lipid membranes formed from POPS/POPC liposomes.[28]

Functionalization of Supported Lipid Membranes with Cholesteryl-TEG-DNA. Finally, cholesteryl-TEG oligonucleotides associated with lipid bilayers on spherical supports were studied. It has been previously reported that a 1:1 lipid mixture of POPS and POPC is able to form homogeneous bilayers on silica particles coated with polyelectrolyte multilayers.[29] Thus, we used flow cytometry to examine the interaction of the oligonucleotides O1, O2, and O3* with this kind of supported lipid membranes. As shown in Figure 9 (panels A and C), no fluorescence signal was observed when the particles were incubated only with the FAM-labeled O3* (no lipophilic anchor), indicating that nonspecific adsorption of DNA on the coated particles was negligible. This result further confirms the high quality of the lipid coating, since otherwise the negatively charged oligonucleotides could bind to the underlaying positively charged polymer. On the other hand, when the particles were sequentially incubated with O1, O2, and O3* (panels B and D), a strong fluorescence was detected, with a signal-to-noise ratio of 102. These results show that the cholesteryl-TEG oligonucleotides were successfully incorporated into the supported lipid bilayers while maintaining their ability to bind cDNA sequences. Furthermore, the narrow peak observed in the fluorescence histogram (coefficient of variation = 6.4) suggests that the lipophilic oligonucleotides are homogeneously distributed among the whole population of lipid-coated particles. To test the stability of the insertion, the same samples were measured again after 24 h storage at 4 °C and 10 extra washing steps with HEPES buffer. The particles retained more than 90% of their initial fluorescence intensity (data not shown).

Discussion

In this study, we combine solid-state NMR, differential scanning calorimetry, confocal fluorescence microscopy, fluorescence lifetime measurements, and flow cytometry to characterize lipophilic oligonucleotides associated with lipid bilayers, free-standing or on polyelectrolyte multilayer particles that can be then easily functionalized for specific targeting. We used the duplex oligonucleotide design as suggested by the Höök group,[10] but a single-stranded DNA molecule with only one cholesterol anchor may also provide sufficient membrane anchorage, as reported recently in the literature[39] and observed also in our study of the lateral distribution of the cholesteryl-TEG oligonucleotides.

First, the lipophilic anchor moiety (cholesteryl-TEG) was studied with regard to the membrane incorporation properties and its influence on the bilayer morphology. The ^{31}P and ^{2}H NMR data clearly show that cholesteryl-TEG is incorporated into the lipid membrane without destroying the bilayer structure or inducing formation of nonlamellar phases. Cholesteryl-TEG only negligibly influences the POPC membrane in contrast to natural cholesterol, which increases the ^{2}H NMR order parameters of lipid membranes to the same extent. It has been shown that the physicochemical properties of various steroid analogues and natural precursors featuring small variations in chemical structure fail to mimic the unique properties of natural cholesterol.[72,73] Cholesterol inserts into lipid membranes with its long axis parallel to the bilayer normal, with the planar ring structure interacting with hydrocarbon chains of lipids and the free polar hydroxyl group pointing toward the membrane surface.[72] Modification of this small "head group" with the large polar TEG moiety may change the orientation and insertion depth of the cholesterol analogue and reduce its condensation ability. Furthermore, it would certainly interfere with the interaction of cholesterol with phospholipids, in particular with PC. According to the "umbrella" model, cholesterol is covered by the rather large headgroup of PC, enabling a strong hydrophobic interaction of the cholesterol backbone with saturated fatty acid chains of PC,[74] although no influence of cholesterol on the structure and dynamics of the PC headgroup is detected.[63] The large TEG moiety may prevent this coverage of the cholesteryl moiety by the PC headgroup.

Second, the spontaneous incorporation of cholesteryl-TEG-DNA oligonucleotides into free-standing lipid membranes was investigated. ^{31}P and ^{2}H solid-state NMR data show that neither the hydrocarbon chains nor the membrane headgroup region are significantly altered by the incorporation of the lipophilic moiety of the oligonucleotide. The isotropic peak in ^{31}P NMR spectra, associated with mobile phosphates of oligonucleotides, showed a slightly increased width after addition of the oligonucleotide complementary to the free 3′-end of O1/O2 duplexes,

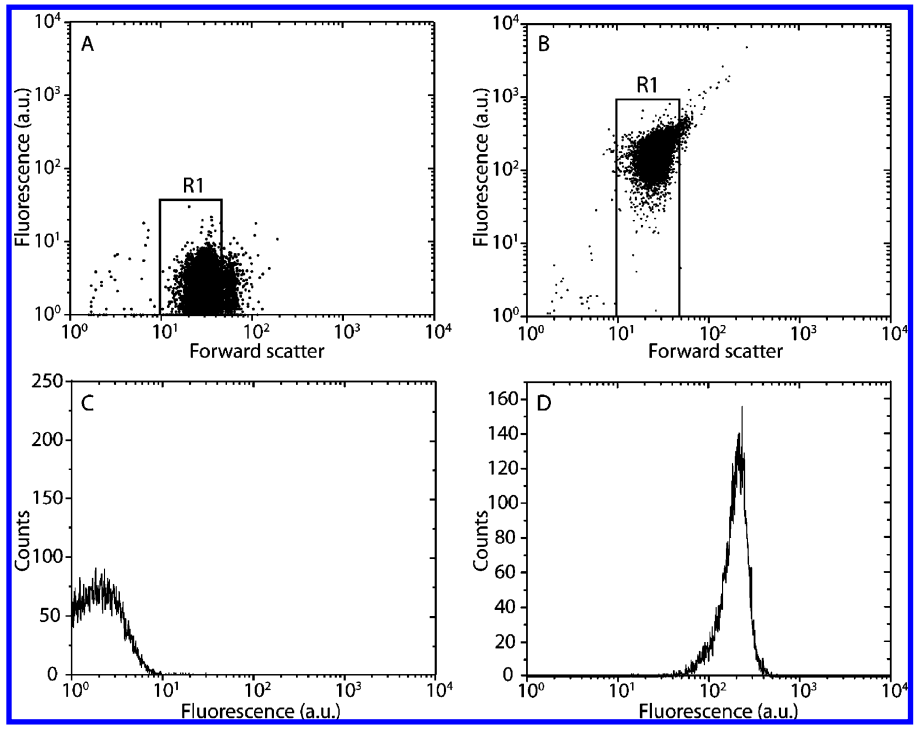

Figure 9. Flow cytometry dot plots and corresponding histograms for 10^4 single lipid-coated particles (region R1): (A, C) particles incubated with FAM-labeled O3* only; (B, D) particles incubated sequentially with O1, O2, and O3*.

which may provide an indication for the molecular recognition event. As indicated by DSC measurements, the stability of the DNA helix is increased in comparison to unmodified oligonucleotides, due to hydrophobic effects that keep the two cholesterol molecules together in the hydrophobic core of the lipid membrane. The lower melting temperature of the duplex at the free 3′- end compared to the T_M of the double-stranded helix with two cholesteryl-TEG modifications has important technological implications: by heating up the sample, the sequences complementary to the free 3′-end can be separated on demand and replaced with modified oligonucleotides carrying fluorophores, antibodies, or peptides. In combination with a particle-based system, such as that provided by supported lipid membranes on LbL-coated colloids, the separation can be achieved through simple centrifugation and redispersion cycles. These advantages open the way for the use of oligonucleotide-functionalized particles as a versatile and reusable tool in pharmacy and nanomedicine.

Third, the lateral distribution of cholesteryl-TEG-DNA in so-called raft membranes was studied. In cell membranes, lipid rafts are enriched in cholesterol and sphingolipids, and cholesterol is known to interact more favorably with sphingolipids than with PC (reviewed elsewhere[75,76]); therefore, we studied the lateral distribution of cholesteryl-TEG oligonucleotides in vesicles made of a physiological lipid mixture of 1:1:1 DOPC: SSM:cholesterol. We found that in this system cholesteryl-TEG-DNA is equally distributed between liquid-ordered and liquid-disordered domains, as proven by confocal fluorescence microscopy and fluorescence lifetime imaging microscopy. Since liquid-ordered domains are enriched in natural cholesterol, it could be reasonably expected that cholesterol-modified molecules would spontaneously incorporate into such domains. Cholesteryl-TEG-DNA complexes failed, however, to segregate in ternary lipid bilayers, probably as a consequence of the physicochemical properties of the cholesteryl-TEG monomer, which behaves differently from natural cholesterol and does not increase the molecular order in lipid membranes. It is known from previous work that cholesterol covalently attached to biomolecules via its free hydroxyl group may lose its ability to partition into liquid-ordered domains.[30] Nevertheless, the cholesteryl anchor allows functionalization of the liquid-ordered domain, which could not be achieved so far by other lipophilic oligonucleotides. Furthermore, in DOPC/DPPC/cholesterol membranes, Beales and Vanderlick[39] have recently observed significantly higher partitioning of cholesteryl-TEG oligonucleotides into liquid-ordered domains.

Finally, we demonstrated the feasibility of using cholesteryl-TEG-DNA for the functionalization of lipid bilayers on layer-by-layer polyelectrolyte-coated spherical supports. The lipophilic oligonucleotides showed a remarkably stable insertion into these supported lipid membranes, while maintaining their specific biorecognition properties. Moreover, the lipid-coated particles did not show any interaction with unmodified oligonucleotides. Since polyelectrolyte multilayers are known to interact nonspecifically with DNA, the coating of the particles with lipid bilayers represents an adequate strategy for the specific incorporation of lipophilic oligonucleotides into a biocompatible and inert surface, avoiding unwanted interaction with other molecules. Thus, the functionalized supported lipid membranes constitute a simple and versatile tool for the development of DNA-based biotechnological, pharmaceutical, and diagnostic applications.

Acknowledgment. P.P. and D.H. are grateful to Dr. Christian Lange (Martin Luther University Halle-Wittenberg) for help with the DSC measurements. This work was supported by a grant from the Federal Ministry of Education and Research (BMBF 0312027 A, C, and D). We thank the DFG (German Research Foundation) and the Experimental Physics Institutes of the University of Leipzig for measuring time on the Avance 750 MHz NMR spectrometer.

Supporting Information Available: Figures showing a typical FLIM picture of a GUV with FAM-labeled O1 inserted into the membrane and a typical fluorescence decay curve of

FAM and the best two-exponential fit. This material is available free of charge via the Internet at http://pubs.acs.org.

References and Notes

(1) Niemeyer, C. M. *Science* **2002**, *297*, 62–63.
(2) Niemeyer, C. M. *Curr. Opin. Chem. Biol.* **2000**, *4*, 609–618.
(3) Aldaye, F. A.; Palmer, A. L.; Sleiman, H. F. *Science* **2008**, *321*, 1795–1799.
(4) Gartner, Z. J.; Bertozzi, C. R. *Proc. Natl. Acad. Sci. U.S.A.* **2009**, *106*, 4606–4610.
(5) Casey, P. J. *Science* **1995**, *268*, 221–225.
(6) Brunsveld, L.; Waldmann, H.; Huster, D. *Biochim. Biophys. Acta* **2009**, *1788*, 273–288.
(7) Milani, S.; Bombelli, F. B.; Berti, D.; Hauss, T.; Dante, S.; Baglioni, P. *Biophys. J.* **2006**, *90*, 1260–1269.
(8) Banchelli, M.; Berti, D.; Baglioni, P. *Angew. Chem., Int. Ed.* **2007**, *46*, 3070–3073.
(9) Milani, S.; Bombelli, F. B.; Berti, D.; Baglioni, P. *J. Am. Chem. Soc.* **2007**, *129*, 11664–11665.
(10) Pfeiffer, I.; Höök, F. *J. Am. Chem. Soc.* **2004**, *126*, 10224–10225.
(11) Beales, P. A.; Vanderlick, T. K. *J. Phys. Chem. A* **2007**, *111*, 12372–12380.
(12) Banchelli, M.; Betti, F.; Berti, D.; Caminati, G.; Bombelli, F. B.; Brown, T.; Wilhelmsson, L. M.; Norden, B.; Baglioni, P. *J. Phys. Chem. B* **2008**, *112*, 10942–10952.
(13) Maru, N.; Shohda, K. I.; Sugawara, T. *Chem. Lett.* **2008**, *37*, 340–341.
(14) Ramirez, F.; Mandal, S. B.; Marecek, J. F. *J. Am. Chem. Soc.* **1982**, *104*, 5483–5486.
(15) Chan, Y. H. M.; van Lengerich, B.; Boxer, S. G. *Proc. Natl. Acad. Sci. U.S.A.* **2009**, *106*, 979–984.
(16) Bunge, A.; Kurz, A.; Windeck, A. K.; Korte, T.; Flasche, W.; Liebscher, J.; Herrmann, A.; Huster, D. *Langmuir* **2007**, *23*, 4455–4464.
(17) Kurz, A.; Bunge, A.; Windeck, A.-K.; Rost, M.; Flasche, W.; Arbuzova, A.; Strobach, D.; Müller, S.; Liebscher, J.; Huster, D.; Herrmann, A. *Angew. Chem., Int. Ed. Engl.* **2006**, *45*, 4440–4444.
(18) Siontorou, C. G.; Nikolelis, D. P.; Tarus, B.; Dumbrava, J.; Krull, U. J. *Electroanalysis* **1998**, *10*, 691–694.
(19) Herbert, B. S.; Gellert, G. C.; Hochreiter, A.; Pongracz, K.; Wright, W. E.; Zielinska, D.; Chin, A. C.; Harley, C. B.; Shay, J. W.; Gryaznov, S. M. *Oncogene* **2005**, *24*, 5262–5268.
(20) Yoshina-Ishii, C.; Boxer, S. G. *J. Am. Chem. Soc.* **2003**, *125*, 3696–3697.
(21) Benkoski, J. J.; Hook, F. *J. Phys. Chem. B* **2005**, *109*, 9773–9779.
(22) Soutschek, J.; Akinc, A.; Bramlage, B.; Charisse, K.; Constien, R.; Donoghue, M.; Elbashir, S.; Geick, A.; Hadwiger, P.; Harborth, J.; John, M.; Kesavan, V.; Lavine, G.; Pandey, R. K.; Racie, T.; Rajeev, K. G.; Rohl, I.; Toudjarska, I.; Wang, G.; Wuschko, S.; Bumcrot, D.; Koteliansky, V.; Limmer, S.; Manoharan, M.; Vornlocher, H. P. *Nature* **2004**, *432*, 173–178.
(23) Stengel, G.; Zahn, R.; Hook, F. *J. Am. Chem. Soc.* **2007**, *129*, 9584+.
(24) Jakobsen, U.; Simonsen, A. C.; Vogel, S. *J. Am. Chem. Soc.* **2008**, *130*, 10462+.
(25) Loew, M.; Kang, L.; Dahne, L.; Hendus-Altenburger, R.; Kaczmarek, O.; Liebscher, J.; Huster, D.; Ludwig, K.; Bottcher, C.; Herrmann, A.; Arbuzova, A. *Small* **2009**, *5*, 320–323.
(26) Johnston, A. P. R.; Cortez, C.; Angelatos, A. S.; Caruso, F. *Curr. Opin. Colloid Interface Sci.* **2006**, *11*, 203–209.
(27) Angelatos, A. S.; Radt, B.; Caruso, F. *J. Phys. Chem. B* **2005**, *109*, 3071–3076.
(28) Bunge, A.; Fischlechner, M.; Loew, M.; Arbuzova, A.; Herrmann, A.; Huster, D. *Soft Matter* **2009**, *5*, 3331–3339.
(29) Fischlechner, M.; Zaulig, M.; Meyer, S.; Estrela-Lopis, I.; Cuellar, L.; Irigoyen, J.; Pescador, P.; Brumen, M.; Messner, P.; Moya, S.; Donath, E. *Soft Matter* **2008**, *4*, 2245–2258.
(30) Wang, T. Y.; Leventis, R.; Silvius, J. R. *Biochemistry* **2001**, *40*, 13031–13040.
(31) Sengupta, P.; Hammond, A.; Holowka, D.; Baird, B. *Biochim. Biophys. Acta* **2008**, *1778*, 20–32.
(32) Baumgart, T.; Hammond, A. T.; Sengupta, P.; Hess, S. T.; Holowka, D. A.; Baird, B. A.; Webb, W. W. *Proc. Natl. Acad. Sci. U.S.A.* **2007**, *104*, 3165–3170.
(33) Veatch, S. L.; Polozov, I. V.; Gawrisch, K.; Keller, S. L. *Biophys. J.* **2004**, *86*, 2910–2922.
(34) de Almeida, R. F. M.; Fedorov, A.; Prieto, M. *Biophys. J.* **2003**, *85*, 2406–2416.
(35) Bunge, A.; Muller, P.; Stockl, M.; Herrmann, A.; Huster, D. *Biophys. J.* **2008**, *94*, 2680–2690.
(36) Bartels, T.; Lankalapalli, R. S.; Bittman, R.; Beyer, K.; Brown, M. F. *J. Am. Chem. Soc.* **2008**, *130*, 14521–14532.
(37) Maru, N.; Shohda, K. I.; Sugawara, T. *Nucleic Acids Symp. Ser.* **2009**, *48*, 95–96.
(38) Stengel, G.; Simonsson, L.; Campbell, R. A.; Hook, F. *J. Phys. Chem. B* **2008**, *112*, 8264–8274.
(39) Beales, P. A.; Vanderlick, T. K. Partitioning of Membrane-Anchored DNA between Coexisting Lipid Phases. *J. Phys. Chem. B* **2009**, *113*, 13678–13686.
(40) Peters, C.; Wolf, A.; Wagner, M.; Kuhlmann, J.; Waldmann, H. *Proc. Natl. Acad. Sci. U.S.A.* **2004**, *101*, 8531–8536.
(41) Ipsen, J. H.; Mouritsen, O. G.; Bloom, M. *Biophys. J.* **1990**, *57*, 405–412.
(42) Oldfield, E.; Meadows, M.; Rice, D.; Jacobs, R. *Biochemistry* **1978**, *17*, 2727–2740.
(43) Martinez, G. V.; Dykstra, E. M.; Lope-Piedrafita, S.; Job, C.; Brown, M. F. *Phys. Rev. E* **2002**, *66*, 050902.
(44) Hope, M. J.; Bally, M. B.; Webb, G.; Cullis, P. R. *Biochim. Biophys. Acta* **1985**, *812*, 55–65.
(45) Angelova, M.; Soleau, S.; Meleard, P.; Faucon, J. F.; Bothorel, P. *Prog. Lipid Res.* **1992**, *89*, 127–131.
(46) Baumgart, T.; Hunt, G.; Farkas, E. R.; Webb, W. W.; Feigenson, G. W. *Biochim. Biophys. Acta* **2007**, *1768*, 2182–2194.
(47) Carmona-Ribeiro, A. M.; Midmore, B. R. *Langmuir* **1992**, *8*, 801–806.
(48) Davis, J. H.; Jeffrey, K. R.; Bloom, M.; Valic, M. I.; Higgs, T. P. *Chem. Phys. Lett.* **1976**, *42*, 390–394.
(49) Sternin, E.; Bloom, M.; MacKay, L. *J. Magn. Reson.* **1983**, *55*, 274–282.
(50) Lafleur, M.; Fine, B.; Sternin, E.; Cullis, P. R.; Bloom, M. *Biophys. J.* **1989**, *56*, 1037–1041.
(51) Huster, D.; Arnold, K.; Gawrisch, K. *Biochemistry* **1998**, *37*, 17299–17308.
(52) Petrache, H. I.; Tu, K.; Nagle, J. F. *Biophys. J.* **1999**, *76*, 2479–2487.
(53) Petrache, H. I.; Dodd, S. W.; Brown, M. F. *Biophys. J.* **2000**, *79*, 3172–3192.
(54) Lakowicz, J. R. *Principles of Fluorescence Spectroscopy*; Springer: New York, 2006; pp 141−143.
(55) Seelig, J. *Biochim. Biophys. Acta* **1978**, *515*, 105–140.
(56) Seelig, J.; Seelig, A. *Q. Rev. Biophys.* **1980**, *13*, 19–61.
(57) Brown, M. F.; Lope-Piedrafita, S.; Martinez, G. V.; Petrache, H. I. Solid-state deuterium NMR spectroscopy of membranes. In *Modern Magnetic Resonance*; Webb, G., Ed.; Springer: Heidelberg, Germany, 2006; pp 241−252.
(58) Brown, M. F. Membrane structure and dynamics studied with NMR spectroscopy. In *Biological Membranes. A Molecular Perspective from Computation and Experiment*; Merz, K. M., Roux, B., Eds.; Birkhäuser: Boston, MA, 1996; pp 175−252.
(59) Gawrisch, K.; Soubias, O. *Chem. Phys. Lipids* **2008**, *153*, 64–75.
(60) Schiller, J.; Müller, M.; Fuchs, B.; Arnold, K.; Huster, D. *Curr. Anal. Chem.* **2007**, *3*, 283–301.
(61) Kaczmarek, O.; Brodersen, N.; Bunge, A.; Loser, L.; Huster, D.; Herrmann, A.; Arbuzova, A.; Liebscher, J. *Eur. J. Org. Chem.* **2008**, 1917–1928.
(62) Brodersen, N.; Li, J.; Kaczmarek, O.; Bunge, A.; Loser, L.; Huster, D.; Herrmann, A.; Liebscher, J. *Eur. J. Org. Chem.* **2007**, 6060–6069.
(63) Brown, M. F.; Seelig, J. *Biochemistry* **1978**, *17*, 381–384.
(64) Stockton, G. W.; Smith, I. C. P. *Chem. Phys. Lipids* **1976**, *17*, 251–263.
(65) Vogel, A.; Katzka, C. P.; Waldmann, H.; Arnold, K.; Brown, M. F.; Huster, D. *J. Am. Chem. Soc.* **2005**, *127*, 12263–12272.
(66) Trouard, T. P.; Alam, T. M.; Brown, M. F. *J. Chem. Phys.* **1994**, *101*, 5229–5261.
(67) Otten, D.; Brown, M. F.; Beyer, K. *J. Phys. Chem. B* **2000**, *104*, 12119–12129.
(68) Breslauer, K. J.; Frank, R.; Blocker, H.; Marky, L. A. *Proc. Natl. Acad. Sci. U.S.A.* **1986**, *83*, 3746–3750.
(69) Duguid, J. G.; Bloomfield, V. A.; Benevides, J. M.; Thomas, G. J. *Biophys. J.* **1996**, *71*, 3350–3360.
(70) Letsinger, R. L.; Chaturvedi, S. K.; Farooqui, F.; Salunkhe, M. *J. Am. Chem. Soc.* **1993**, *115*, 7535–7536.
(71) Veatch, S. L.; Keller, S. L. *Biophys. J.* **2003**, *85*, 3074–3083.
(72) Scheidt, H. A.; Muller, P.; Herrmann, A.; Huster, D. *J. Biol. Chem.* **2003**, *278*, 45563–45569.
(73) Endress, E.; Heller, H.; Casalta, H.; Brown, M. F.; Bayerl, T. M. *Biochemistry* **2002**, *41*, 13078–13086.
(74) Huang, J. Y.; Feigenson, G. W. *Biophys. J.* **1999**, *76*, 2142–2157.
(75) Jacobson, K.; Mouritsen, O. G.; Anderson, R. G. W. *Nat. Cell Biol.* **2007**, *9*, 7–14.
(76) Fullekrug, J.; Simons, K. *Ann. N.Y. Acad. Sci.* **2004**, *1014*, 164–169.

JP9067747